10th Int. Cold Forging Congress 2000
Sept 13-15, 2000 - Stuttgart

430

Prediction and Elimination of Defects in Cold Forging Using Process Simulation

Taylan Altan, Professor & Director, ERC for Net Shape Manufacturing, Columbus, OH, USA
Dan Hannan, Graduate Research Associate, ERC for Net Shape Manufacturing, Columbus, OH, USA

1. Introduction

In the automotive industry, many shaft and shaft-like components, including fasteners, are produced by forward extrusion. Some of these components are considered critical for the safe performance of the vehicle and must be free of defects. These defects could be visible external ones, such as laps or cracks, or non-visible internal defects, such as chevrons. See Figures 1 and 2 for examples of chevron defects.

The objectives of the study described in this paper are to demonstrate how to:

- Measure critical damage values for typical materials used in cold extrusion
- Develop criteria or guidelines for designing forward extrusion dies for producing chevron-free extrusions.

2. Process Modeling

Process modeling is used in cold forging to predict metal flow, stress and temperature distributions, stresses and forces exerted on tools, and potential sources of defects and failures. In some cases, it is even possible to predict product microstructure and properties as well as elastic recovery and residual stresses /1,2/.

Figure 1. Automotive axle shaft with chevrons

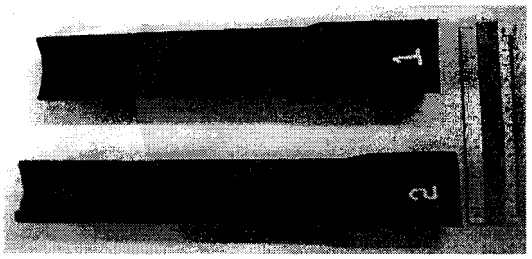

Figure 2. Illustration of different chevron configurations

The main objectives of process modeling in forging are to:

a) Develop adequate die design and establish process parameters by:

- Predicting metal flow and final dimensions of the formed part

- Preventing flow induced defects such as laps and cold shuts
- Predicting processing limits that should not be exceeded so that internal and surface defects are avoided,
- Predicting temperatures so that part properties, friction conditions, and die life can be controlled

b) Improve part quality and complexity while reducing manufacturing costs by:

- Predicting and improving grain flow and microstructure
- Reducing die try-out and lead times
- Reducing rejects and improving material yield

The steps involved in integrated product and process design for massive forming are schematically illustrated in Fig. 3. Based on functional requirements, the geometry (shape, size, surface finish, tolerances) and the material are selected for a part at the design stage. It is well known that the design activity represents only a small portion, 5 to 15 percent, of the total production costs of a part. However, decisions made at the design stage determine the overall manufacturing, maintenance, and support costs associated with a specific product. Once the part is designed for a specific process, the steps outlined in Fig. 3 lead to a rational process design.

3. Simulation of Forging Processes

Several issues, such as material properties, geometry representation, computation time, and remeshing capability, must be considered in cost effective and reliable application of numerical process modeling.

3.1 Geometry

Depending on its geometrical complexity, a forging process can be simulated either as a two dimensional, axisymmetric or plane strain, or a three dimensional problem. In general, in order to have an efficient simulation it is necessary to remove all minor geometrical features, like small radii in the dies /2/. These features do not have a significant effect on the metal flow. However, in some specific applications like microforming processes the size effects should be taken into account in the simulation /3/.

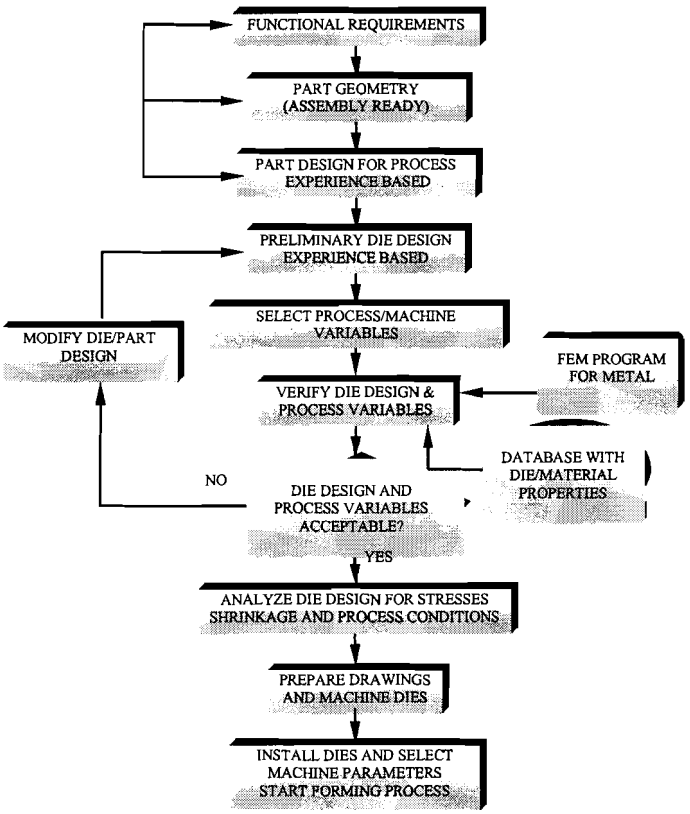

Figure 3. Product & Process Design for Net Shape Manufacturing

3.2 Mesh and Remesh

In massive forming processes the workpiece generally undergoes large plastic deformation, and the relative motion between the deforming material and the die surface is significant. In the simulation of such processes the starting mesh is well defined and can have the desired mesh density distribution. As the simulation continues, the distortion of the workpiece mesh is significant. Hence, it is necessary to generate a new mesh and interpolate the data from the old mesh to the new mesh in order to obtain accurate results /4/. The mesh density should conform to the geometrical features of the workpiece at each step of deformation /5/. These capabilities are available in commercial codes used in industrial practice.

3.3 Workpiece and Tool Material Properties

In order to accurately predict the metal flow and the forming loads it is necessary to use reliable input data. The stress-strain relation or flow curve is generally obtained from a compression test. However, this test is limited in the amount of achievable strains.

In most simulations the tools are considered rigid, thus, die deformation and stresses are neglected. However, in precision forging operations, the relatively small elastic deformations of the dies may influence the thermal and mechanical loading conditions and the contact stress distribution at the die-workpiece interface. Knoerr, Lange and Altan /6/ presented a concept in which the data generated from the process simulation is used to perform the stress and fatigue analysis of an arbitrary die. Most commercial codes have the capability to perform stress analysis of the tooling. However, these are not able to perform fatigue analysis

due to both the complexity of the analysis and the scarcity of fatigue data for tooling materials.

3.4 Interface Conditions (Friction and Heat transfer)

The friction and heat transfer coefficients are not readily available in literature. Thus, it is necessary to measure them for process conditions as close as possible to the actual production process. In hot and warm forging the constant shear friction factor is determined by a ring compression test, while in cold forging it is recommended to perform a double backward extrusion test /7-10/. This choice is made because surface generation and tool pressures are generally higher in cold forging than in hot and warm forging.

To determine the heat transfer coefficient an upsetting tooling must be instrumented with several fast response thermocouples at known distances from the surface. Then simulations are performed to match the temperature distribution of the experiments by varying the heat transfer coefficient /7/.

3.5 Characteristics of the Simulation Code (Reliability and Computation Time)

Several commercial codes are available for numerical simulation of forging processes; such as DEFORM™ 2D, DEFORM™ 3D, FORGE™ 2 and FORGE™ 3, Superforge, Autoforge. The accurate and efficient use of metal flow simulations require not only a reliable FE solver /11/, but also:

(i) Software packages for (a) interactive pre-processing to provide the user with control over the initial geometry, mesh generation and the input data; (b) automated remeshing to allow the simulation to continue when the distortion of the old mesh is excessive; and (c) interactive post-processing that provide more advanced data analysis, such as point tracking and flow line calculation.

(ii) Appropriate input data describing (a) thermal and physical properties of die and billet material; (b) heat transfer and friction at the die-workpiece interface under the processing conditions being investigated; and (c) flow behavior of the deforming material at the relatively large strains that occur in practical metal forming operations.

(iii) Analysis capabilities that are able to (a) perform the process simulation with rigid dies to reduce calculation time; and (b) use contact stresses and temperature distribution from the process simulation with rigid dies to perform elastic plastic die stress analysis.

4. Ductile Fracture

Ductile fracture can be defined as a fracture that occurs after a component experiences a significant amount of plastic deformation /12/. Fracture is influenced by numerous parameters including the deformation history of the workpiece material and the process conditions (i.e. rate of deformation, lubrication, and friction) /13/. Other factors that influence fracture include chemical composition, microstructure, surface conditions, and homogeneity. Several ductile fracture criteria are useful for predicting surface or internal cracks. These can be generally represented by:

$$\int F(deformation)d\bar{\varepsilon} = C \qquad (1)$$

Equation 1 means that ductile fracture is a function of the plastic deformation history and properties of the material. These include the geometry, damage value, *C*, and strain of the workpiece (or effective strain), $\bar{\varepsilon}$. When the maximum damage value (MDV) of the material exceeds the critical damage value (CDV), crack formation is expected. Different ductile fracture criteria yield different damage values for a given process /14/.

Kim /14/ reviewed the literature and developed a methodology to predict ductile fracture by using FE simulations (see Figure 4). It was found that the modified Cockroft and Latham's criterion predicts, with good agreement, the location of the maximum damage value /15/. Also predicted is that fracture occurs when the cumulative energy, C, due to the maximum tensile stresses, σ^*, exceeds a certain value (Equation 2):

$$\int_{\bar{\varepsilon}} \frac{\sigma^*}{\bar{\sigma}} d\bar{\varepsilon} = C_b \qquad (2)$$

Cerretti /13/ further developed the methodology to simulate the fracture of components subjected to large amounts of deformation and simulated sucessfully the formation of chevron cracks for the extrusion experiments performed by Kim /14/. The results are seen in Figure 5. This algorithum is now incorporated into the FEM code DEFORM™ and used for predicting the probability of internal and external fractures in cold forging operations.

5. Methodology to Predict Ductile Fracture

Assuming the CDV is a material constant, several tests should be performed to obtain, for a given material, the flow stress and the critical damage value (CDV), as shown in Figure 4. Once the CDV for a specific material is obtained it is possible to predict through FEM simulations the formation of cracks in forming operations.

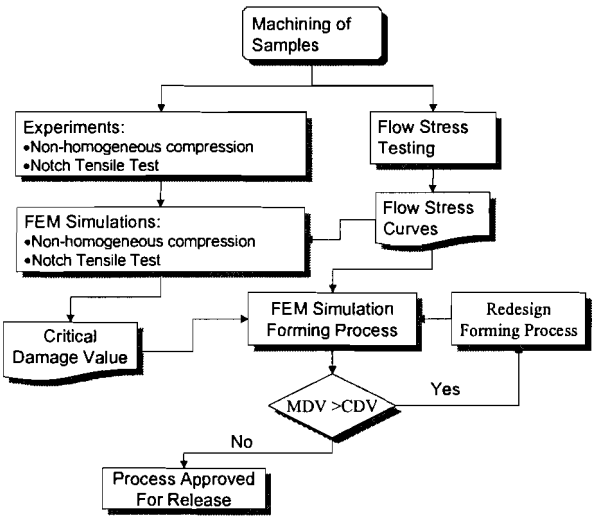

Figure 4. Methodology to predict & prevent the formation of cracks in metal forming operations

Two different materials were selected for this study: SAE 1524 (spheroidized), which is a high-manganese carbon steel and SAE 1137 (hot rolled), which is a resulfurized carbon steel. The SAE 1137 material was produced as a coarse grain product, making it more likely to crack. The actual chemical composition, in percent (%) of these steels are shown in Table 1.

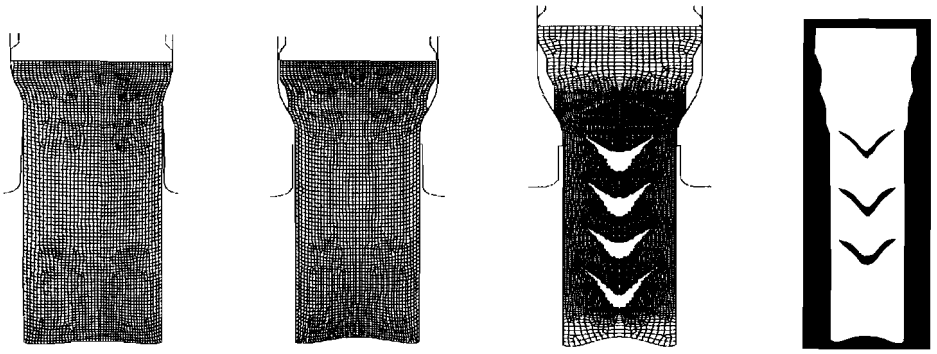

Figure 5. Simulation of a) first, b) second, and c) third pass forward extrusion. The actual product (d) is also shown

SAE	C	Mn	P	S	Si	Cu	Sn	Ni	Mo	Cr	As	Cb	V	N	Al
1524	0.22	1.35	0.04	0.05	0.15	---	---	---	---	---	---	0.02	---	---	0.015
1137	0.39	1.48	0.013	0.1	0.16	0.17	0.01	0.06	0.02	0.08	0.005	0.001	0.01	0.004	0.004

Table 1. Chemical composition (in %) for SAE 1524 (spheroidized) and SAE 1137 (hot rolled).

5.1 Measurement of Critical Damage Value (CDV)

The critical damage values were obtained by two tests; a non-uniform compression test with grooved dies and a tensile test with a notched specimen. The non-uniform compression test with grooved dies consists of upsetting a cylinder until a crack is detected near the equatorial surface. The specimen height at which the crack occurs is known as the fracture height, H_f. Then FE simulations are conducted for the compression test up to the fracture height, H_f, to obtain the distribution of the damage value in the workpiece at the time of fracture. In this study, the damage value was obtained by using equation 2. The maximum damage value (MDV) is the critical damage value (CDV) of the material tested.

The non-homogeneous compression tests with grooved dies were conducted with cylindrical specimens to produce cracks on the free or bulged surface. In these tests, the 1.5 in (38.1 mm) high samples were upset in .040 in (1 mm) increments of deformation. At each deformation step the bulged surface of the specimen was inspected for cracks. The fracture height, H_f, was identified as the specimen height where a crack was first visible. The results from these tests are as follows (see Figure 6):

- Vertical cracks were seen in the equatorial surface of the specimens.
- Fractures were observed in SAE 1137 at a lower reduction in height than in SAE 1524.
- At the moment of crack formation, SAE 1524 showed a more sudden tensile failure than 1137.

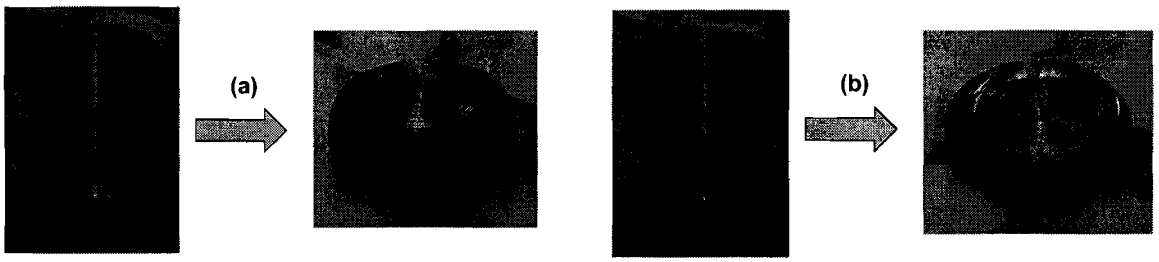

Figure 6. Specimens for non-uniform compression test; a) SAE 1137 hot rolled, b) SAE 1524 spheroidized annealed

In the tensile test with a notched specimen, the neck diameter is measured continuously until the specimen fractures. Then simulations are conducted to calculate the damage distribution at the instant the neck diameter reaches the fracture diameter, d_f. The MDV determined just before fracture is the CDV. Tensile tests were conducted to provide information on the average fracture strain at the neck cross section obtained from load vs. neck diameter

curves. The tests were performed at the Mechanical Behavior Laboratories at the Ohio State University. An INSTRON Model 1322 servo hydraulic press, capable of pulling 55,000 pounds, was used. During the tests the following information was recorded:

- Neck diameter at fracture (with the help of a clip gage).
- Elongation of the specimen (with extensometer). The gage length of the specimen was 1 inch.
- Tensile force using a load cell

The fracture found in the tension specimens was a cup-and-cone type. This indicates that the fracture begins at the center of the notched specimen. Curves for the load vs. neck diameter for both materials are given in Figure 7. The elongation of the specimen and the reduction of the neck diameter are higher for SAE 1524, indicating higher ductility.

5.2 Calibration of the Critical Damage Value through Process Simulation

The calibration using FEM analysis was conducted up to the fracture height, H_f, for the compression tests with grooved dies; and up to the final neck diameter for the notched tensile test. The critical damage values obtained from the simulations for both non-homogeneous compression and notched tensile tests are given in Table 2. The critical damage values for the notched tensile tests are different than the ones obtained from the compression tests with grooved dies. One logical explanation for the difference between compression and tension is the ability to detect the initiation of the crack. During the tensile test, the crack starts at the center and is not visible. For the compression test, the sensitivity of detecting the crack is in increments of .040 in. (1mm) of ram movement. Therefore, the determination of the CDV at a given reduction in height is within a certain margin of error, i.e. the height at which CDV is given may be up to 1mm smaller than the height where the crack actually occurred.

Another possible reason for the difference in the CDV's obtained in tensile and compression tests is that the state of stress is different for each case. In order to use a CDV in practical process evaluations, the average CDV value obtained from the compression and tensile tests was used.

The simulations coincide with the experiments with respect to the location of the CDV as shown in Figure 8. The location of the CDV during the compression with grooved dies is at the equatorial surface, while on the notch tensile test it is at the center of the notched specimen.

Material	Method	CDV	Location
SAE 1137	compression with grooved dies	0.37	equatorial surface
	notch tensile test	0.35	center of specimen
SAE 1524	compression with grooved dies	0.65	equatorial surface
	notched tensile test	0.675	center of specimen

Table 2. CDV's obtained during FEM Calibration

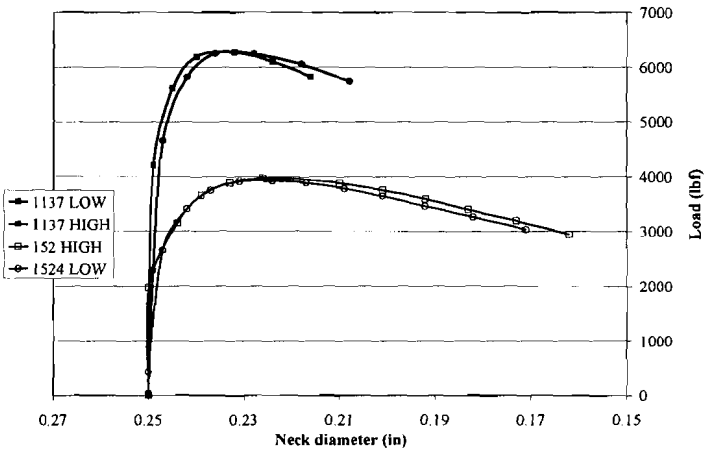

Figure 7. Neck diameter-load curve for tensile tests with notched specimens of SAE 1137 hot rolled and SAE 1524 spheroidized annealed.

The simulations coincide with the experiments with respect to the location of the CDV as shown in Figure 8. The location of the CDV during the compression with grooved dies is at the equatorial surface, while on the notch tensile test it is at the center of the notched specimen.

6. Evaluation of the Forward Extrusion Process with Spherical Dies

The objectives of the parametric study were (See Figure 9) to determine:

- The effect of the die land length, B, on damage value
- The likelihood of forming chevrons for a die radius, r_d, at reductions in area between 30% to 75%
- The effect of the transition radius, r, on damage value

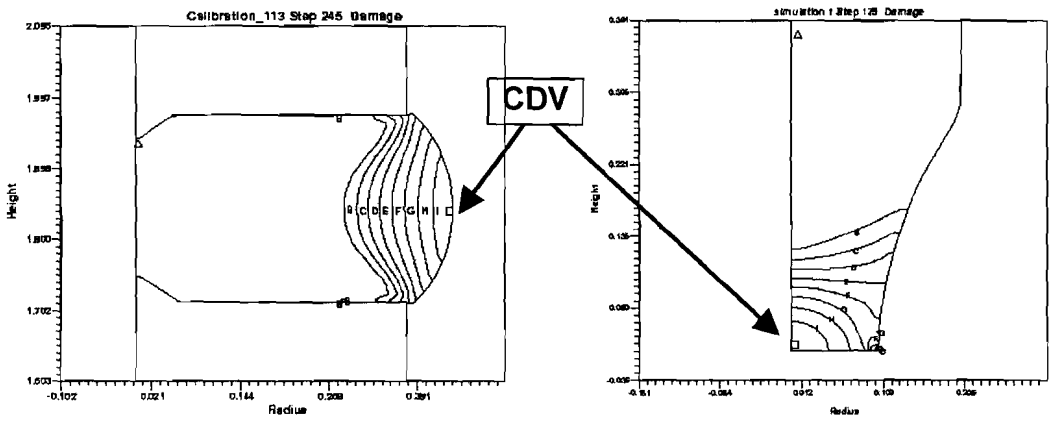

Figure 8. Distribution of the critical damage value for material SAE 1137 (hot rolled) a) non-homogeneous compression and b) notched tensile test.

Forward extrusion simulations were performed to determine the range of process parameters that assure chevron free forward extrusions. The FEM code DEFORM 2D was used for this purpose. The following are a set of initial values:

$2R_0$ = entrance (bore) diameter (1 in.)

$2R_f$ = exit (die) dia.

B = die land length: 0.060 to 0.150 in.

RR = Reduction ratios: 30%, 45%, and 55%

r_d = die radius

r = transition radius: 0.005 in., 0.200 in, 0.300 in.

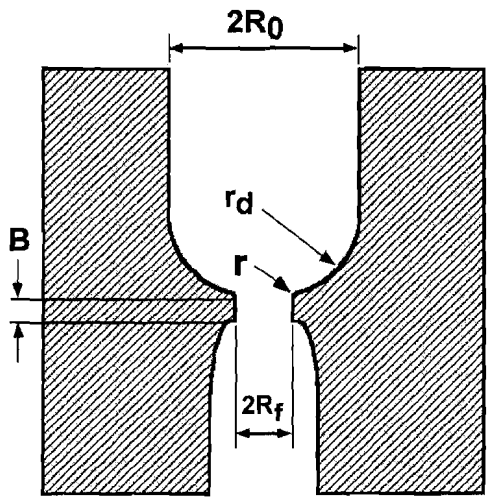

Figure 9. Schematic representation of the parameters to be investigated during forward extrusion with spherical die.

The punch speed was 0.27in/s, with a friction coefficient of m = 0.08. The billet diameter was 1 inch and the billet length was 2 inches. The material selected for the simulations was SAE 1137 hot rolled because it shows less ductility than SAE 1524 spheroidized annealed. This means that SAE 1137 can develop chevron cracks at an earlier stage.

7. Damage Value Prediction for Single-pass Extrusion

Figure 10 shows the variation of the maximum damage value estimated through simulations for one pass extrusion at several reduction ratios. The material used was SAE 1137. In all simulations the maximum damage value is located along the center of the work piece. The highest damage value was 0.33, which does not exceed the selected average CDV of 0.36 for SAE 1137. Therefore, under the selected process conditions, chevron cracks would not be expected during one-pass forward extrusion.

Figure 10 also shows that the effect of the die land length (B) is essentially negligible. When the small transition radius (r = 0.005") is used, there is a higher stress concentration and, therefore, the flow of the material is restricted. The variation of the damage value for the given transition radius, r, is seen in Figure 11. This shows that damage value decreases when the transition radius is increased, especially for reductions in area between 45-55%.

The lowest damage values obtained were at the highest reduction in area evaluated. Notice that as the reduction in area increases, the deformation near the center of the work piece becomes more compressive and DV decreases (see Figure 12 for the distribution at 30%,

45%, and 55%).

8. Damage Value Prediction for Multi-pass Extrusion

The multi-pass extrusion sequence used by Kim /14/ was used in order to validate the premise that the critical damage value can predict the formation of chevron cracks for SAE 1137. The dimensions of the three die inserts used in these simulations are shown in Table 3.

This sequence was selected because, in earlier studies /14/ the products extruded at the same area reduction ratios and half die angle developed chevron cracks. After the first pass of the forward extrusion simulation with conical dies, the damage value obtained was 0.25. During the first pass with spherical dies, the damage value obtained was 0.24. The chevron cracks and the damage distribution can be seen in Figure 13 after the third pass.

The multi-pass forward extrusion simulations showed that the damage value at the center of the work piece will be much higher than using single-pass extrusion, which leads to higher possibility of chevron cracks. This result showed that the CDV for SAE 1137 and the Cockroft and Latham ductile fracture criteria is capable of predicting chevron defects during three-pass forward extrusion.

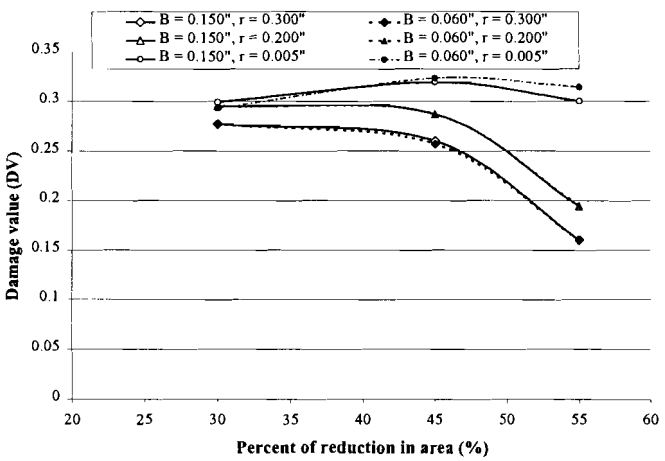

Figure 10. Effect of reduction ratio on damage value in single-pass forward extrusion

Die Insert #	Bore Dia. (in)	Exit Dia. (in)	Die Land Length (in)	Die Angle
1	1.04	0.896	0.125	22
2	1.05	0.826	0.143	22
3	1.06	0.742	0.146	22

Table 3. Die design parameters for forward extrusion with conical dies

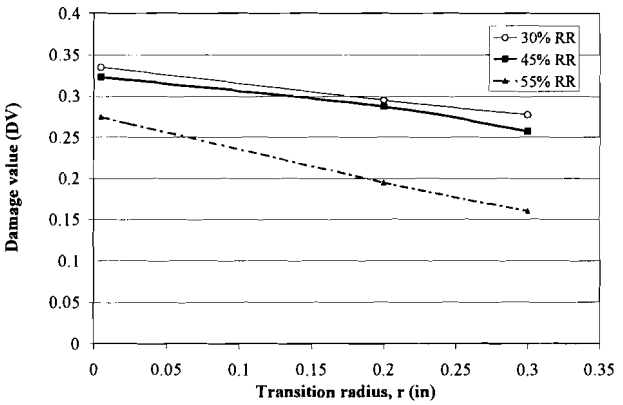

Figure 11. Effect of transition radius on Damage value for several reduction ratios

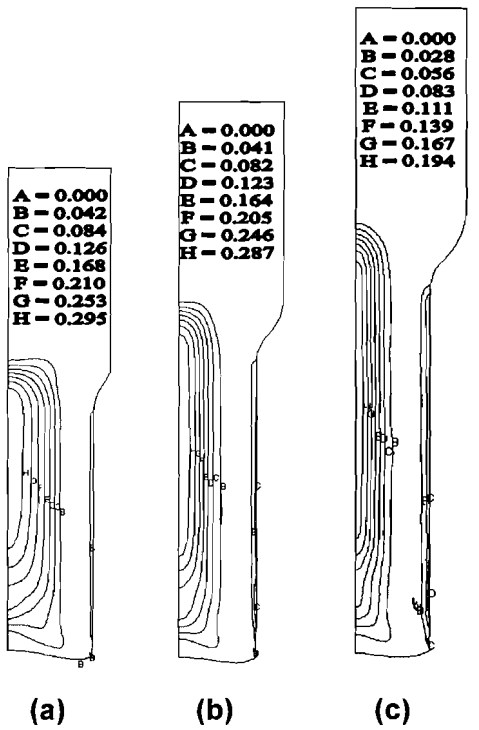

Figure 12. Distribution of the damage value during several reductions in area: (a) 30%, (b) 45% and (c) 55% (B=0.150" and R = .200").

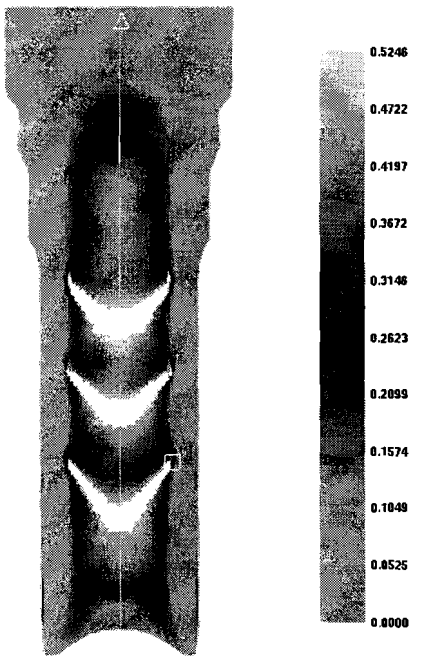

Figure 13. Formation of chevron cracks during three-pass forward extrusion using first pass as spherical die with material SAE 1137 (hot rolled) and its correspondent

9. Conclusions

- Additional refinement in the procedure for detecting crack initiation in the physical testing procedure will improve the accuracy of predicting defects.
- In the forward extrusion simulations using spherical dies the damage value decreases as reduction in area (RA) increases. The damage value decreases when the transition radius is increased, especially for reductions in area between 45-55. The die land length, B, does not have a significant impact on the MDV.
- None of the maximum damage value (MDV) obtained from simulations for single-pass extrusions exceeded the CDV obtained experimentally for SAE 1137 hot rolled. This means that no chevron cracks will form for the selected process conditions.

- The multi-pass forward extrusion simulations show that the damage value at the center of the work piece will be much higher than the damage value predicted using one-pass extrusion. This leads to a higher possibility of chevron cracks in multi-pass extrusion.

- The CDV used for the materials tested is the average value obtained for non-homogeneous compression and notched tensile testing.

- For the same reduction in a single-pass extrusion, a conical die design has a slightly higher damage value (0.25) than a spherical design (0.24). However, this difference is negligible.

In summary, the Critical Damage Value (CDV) concept can be used to predict the possibility of fracture formation in cold extrusion. Thus, using this concept and FEM simulation, die design and process sequence can be modified to avoid fracture defects in cold extrusion.

10. References

/1/ Altan, T., Oh, S.I., and Gegel, H. Metal Forming-Fundamentals and Applications, book published by American Society of Metals (ASM) (1983)

/2/ Altan, T., Oh, S.I. Application of FEM to 2-D Metal Flow Simulation: Practical Examples, Advanced Technology of Plasticity, vol. 4, p. 1779 (1990)

/3/ Messner, A., Engel, U., Kals, R., and Vollertsen, F. Size Effect in the FE Simulation of Microforming Processes, Journal of Materials and Processing Technology, vol. 45, p. 374 (1994)

/4/ Wu, W.T., S.I. Oh, T. Altan, R. A. Miller, Automated Mesh Generation for Forming Simulation-I, Proceedings of ASME International Computers in Engineering, vol. 1, p. 507, Boston, MA. (1991)

/5/ Wu, W.T., Oh, S.I., Altan, T., and Miller, R.A. Optimal Mesh Density Determination for the FEM Simulation of Forming Processes, NUMIFORM '92, September 14-18, 1992, France (1992)

/6/ Knoerr, M., Lange, K., and Altan, T. Fatigue Failure of Cold Forging Tooling: Causes and Possible Solutions Through Fatigue Analysis, Journal of Materials Processing Technology, vol. 46, no. 1-2, p. 57 (1994)

/7/ Burte, P., Semiatin, S.L. and Altan, T. An Investigation of the Heat Transfer and Friction in Hot Forging of 304SS and Ti-6A1-4V. Transactions of North American Manufacturing Research Institution of SME, p. 59, Dearborn, Michigan (1990)

/8/ Bay, N., Wibom, O., and Nielsen, J.A. A New Friction and Lubrication Test for Cold Forging, Annals of CIRP, vol. 44, p. 217. (1995)

/9/ Buschhausen, A., Weinmann, K., Lee, J.Y., and Altan, T., Evaluation of Lubrication and Friction in Cold Forging Using Double Backward Extrusion Process, Journal of Materials and Processing Technology, vol. 33, p. 95. (1992)

/10/ Bennani, B., and Bay, N. Limits of Lubrication in Backward Can Extrusion: Analysis by the Finite Element Method and Physical Modeling Experiments, Proceedings of the 27th ICFG Plenary Meeting, p. 7.1, Padova, Italy (1994)

/11/ Knoerr, M., Lee, J., and Altan, T. Application of the 2D Finite Element Method to Simulation of Various Forming Processes, Journal of Materials Processing Technology, vol. 33, no. 1-2, p. 31,(1992)

/12/ Hosford, W. and Caddell, R. "*Metal Forming: Mechanics and Metallurgy*". Second Edition. PTR Prentice Hall, Englewood Cliffs, N.J. 07632

/13/ Cerretti, E., Taupin, E., Altan, T. "*Simulation of metal flow and fracture applications in orthogonal cutting, blanking and cold extrusion.*" Annals of the CIRP, Vol. 46/1/1997

/14/ Kim, H., Yamanaka, M., Altan, T, Ishii, K. " *Effects of design and process parameters upon the formation of chevron defects in forward rod extrusion*" Engineering research center for the Net Shape Manufacturing. Report No. ERC/NSM-94-41. August 1994.

/15/ OH, S. I., Chen, C., and Kobayashi, S.,(1979) Ductile fracture in Axisymmetric Extrusion and Drawing: Part 2 Workability in Extrusion and Drawing, Transactions of the ASME, 101, Feb. pp.36-44